STUDY OF FUNDAMENTAL SYMMETRY BREAK UP IN *P*-RESONANCE REGIONS

S.B. Borzakov[1], Yu.M. Tchuvil'sky[2]

[1]*Joint Institute for Nuclear Research, 141980, Dubna, Russia*
[2]*Skobeltsyn Institute of Nuclear Physics, M S U, 119991, Moscow, Russia*

Abstract. Long and, unfortunately, unfinished by any result story of well known lanthanum experiment, which was considered as optimal tool of search for ***PT***-noninvariance in nuclear processes, from the idea to an actual measurement make it reasonable to analyze other possibilities provided by neutron induced nuclear reactions. The prospects of search for ***PT***-noninvariant effects in other experiments with neutrons of resonance energy are discussed. Various schemes of ***PT***-nonconserving correlations of the reaction products measurements, which differ in number of vectors involved, method of orientation, method of polarization observation, are analyzed.

MOTIVATION

Nonconservation of discrete fundamental symmetries in physics.

If the CPT-theorem is valid there are four terms in Grand Lagrangian which are distinguished by their discrete fundamental symmetry properties. They are presented in the table 1.

Table 1. Symmetric and symmetry breaking terms of Grand Lagrangian.

C	P	T	Comment 1	Comment 2
+	+	+	Invariant	
–	–	+	P-odd, T-invariant (P)	
–	+	–	P-even, T-noninvariant (T)	CP-noninvariant terms
+	–	–	P-odd, T-noninvariant (PT)	

P-, T-, and PT-noninvariant amplitudes shape the complete set of discrete fundamental symmetry breaking terms of Grand Lagrangian. The first one is leading symmetry breaking term. It is relatively well studied in a lot of parity violation measurements.

Up to now a ***CP***-violation effects (both ***P***-even and ***P***-odd) are observed in the decays of K- [1] and B-mesons [2] only. In the Standard Model (SM) the amplitude of the discussed effects are very small and turn out to be visible due to unique enhancement takes place in the mentioned decays. These amplitudes are described by Cabibbo-Kobayashi-Maskawa matrix:

$$\begin{pmatrix} d' \\ s' \\ b' \end{pmatrix} = \begin{pmatrix} c_1 & \mathrm{s}_1\,\mathrm{c}_3 & \mathrm{s}_1\,\mathrm{s}_3 \\ -s_1\,\mathrm{c}_2 & \mathrm{c}_1\,\mathrm{c}_2\,\mathrm{c}_3 - \mathrm{s}_2\,\mathrm{s}_3\,e^{i\delta} & \mathrm{c}_1\,\mathrm{c}_2\,\mathrm{s}_3 + \mathrm{s}_2\,\mathrm{c}_3\,e^{i\delta} \\ -\mathrm{s}_1\,\mathrm{s}_2 & \mathrm{c}_1\,\mathrm{s}_2\,\mathrm{c}_3 + \mathrm{c}_2\,\mathrm{s}_3\,e^{i\delta} & \mathrm{c}_1\,\mathrm{s}_2\,\mathrm{s}_3 - \mathrm{c}_2\,\mathrm{c}_3\,e^{i\delta} \end{pmatrix} \begin{pmatrix} d \\ s \\ b \end{pmatrix}, \qquad (1)$$

in which the notations $c_i = \cos\vartheta_i$, $s_i = \sin\vartheta_i$ are used, ϑ_i are mixing angles. The phase shift δ is the sole parameter of the SM determining the values of the discussed break up terms. There is no another way to involve CP-nonconservation in the SM. The extremely small measured values of the effects result in some problems in explanation of the absence of

antimatter in the Universe. For this reason it is assumed that a major contributor to these effects is something beyond the SM and related to a new physics. Some models predict rather large effects. Therefore search for ***CP***-nonconserving amplitudes which are essentially larger than the ones predicted by the SM in other processes makes sense.

It should be noted that the phase shift δ is not related to the systems consisting of quarks of the first generation (***u*** and ***d***). That is why nuclear systems are interesting objects of the discussed investigations.

Upper limits of permanent electric dipole moments (PEDM) of elementary particles and atoms are the most informative data concerning the ***PT***-noninvariant effect in light-quark systems up to now. In the framework of SM only second order diagrams presented in fig.1 contribute in PEDM value.

Recent upper limits of PEDM of elementary particles and atoms are presented in the table 2.

It can be concluded from this table that some measurements of PEDM directly impact on construction of the new theoretical approaches. Thus an analysis of alternative schemes promising for setting upper limits on CP-violating effects and, in particular, on ***PT***-noninvariant amplitudes in nuclei seems to be promising.

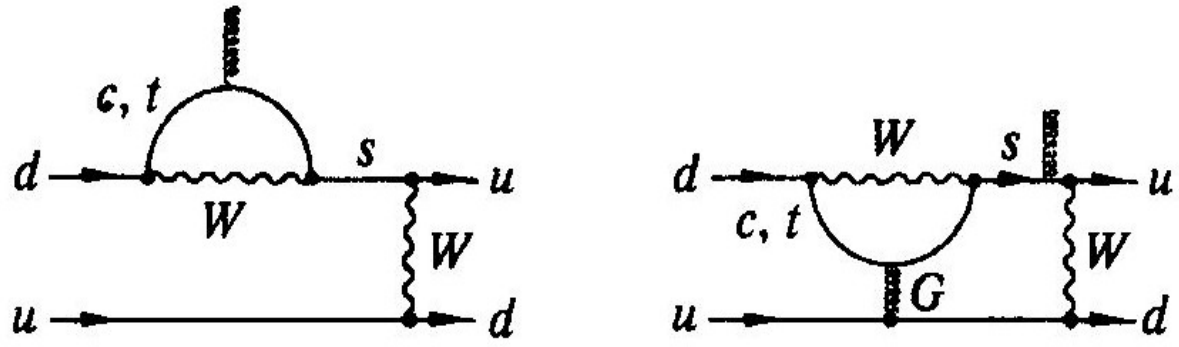

Figure 1. PEDM-producing diagrams of SM. W and G denotes W-boson and gluon respectively.

Table 2. PEDM values of microobjects.

	Experiment (10^{-13} e · cm)	Standard Model (10^{-13} e · cm)	New physics (10^{-13} e · cm)
e	$1.6 \cdot 10^{-14}$	$\leq 10^{-25}$	$\leq 1 \cdot 10^{-14}$
p	$1.0 \cdot 10^{-9}$	$\sim 10^{-18}$	$\leq 6 \cdot 10^{-13}$
n	$2.9 \cdot 10^{-13}$	$\sim 10^{-18}$	$\leq 3 \cdot 10^{-13}$
^{199}Hg	$2.1 \cdot 10^{-15}$	$\sim 10^{-20}$	$\leq 2 \cdot 10^{-15}$

Nuclear processes as tests on *PT*-violation.

It is important to note that the list of amplitudes involved in ***PT***-nonconserving nuclear processes does not limited by that contributing PEDM. So search for the effects here is anyway interesting independently on their compatibility with PEDM approach.

If, nevertheless, one intends to compete and believes that PT-violation effect display itself only in $N \rightarrow N + \pi$ vertex (see the diagram in the fig. 2) then neutron PEDM

measurements set the following constrains on the ***PT***-nonconservation constants of the diagram in the fig. 2:

$$g_{pt}^{\Delta T} \le \begin{Bmatrix} 0.7\cdot 10^{-11} & \Delta T = 0 \\ 0.5\cdot 10^{-10} & \Delta T = 1 \\ 0.7\cdot 10^{-11} & \Delta T = 2 \end{Bmatrix}, \qquad (2)$$

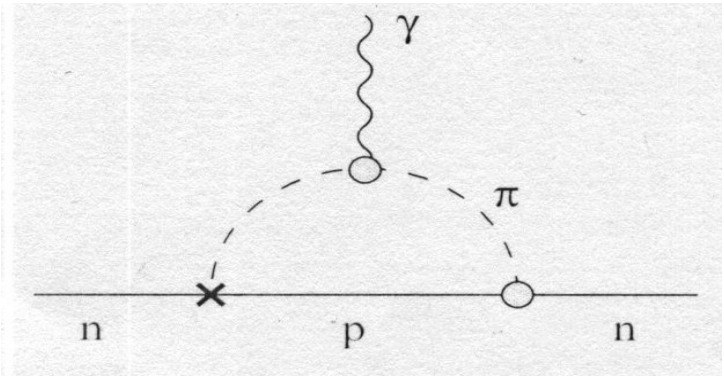

*Figure 2. Diagram producing PEDM of neutron. The cross denotes **PT**-nonconserving vertex.*

where **Δ*T*** is the isospin change. So to compete with these measurements one should achieve a similar precision if only for isovector constant. Fortunately nucleus is an amplifier of isovector effects.

Principal features of the ***PT***-nonconservation studies in nuclear processes and variety of promising experimental schemes of them are discussed in [1]. In the present talk we restrict the discussion by two brief remarks.

The basic condition to obtain a low upper limit of a PT-noninvariant effect is sufficiently large P-violation effect in the chosen example. The greater P-odd effect, the tighter constraints on PT-nonconservation constants may be attained due to a close similarity of P- and PT-nonconserving amplitudes. It may be said that PT-noninvariant amplitude is the real part of the P-odd one which is dominantly imaginary. The examples of objects promising for search for the PT-nonconseration effects should display strong P-violation properties or these properties should be expected.

Search for PT-noninvariant effects in γ-transitions is preferable because otherwise, for strong and/or Coulomb interacting particles, false effect producing by a final state interaction is too large and the T-invariant P-odd amplitude together with the final (or sometimes initial) state interaction will simulate the effect under discussion.

The most successful nuclear experimental result in the ratio of the upper limit of the ***PT***-noninvariant effect $\tilde{a}_{pt}$ to the measured ***P***-odd one a_p $Q = \tilde{a}_{PT} / a_P$ which is equal ~1 for ^{180m}Hf decay [2] and $4.0\cdot 10^{-2}$ for ^{119m}Sn decay [3] – see [2, 3] and related comments in [1].

In the present talk we concentrate on the discussion of ***PT***-nonconservation effects in (n,γ)-reactions induced by neutrons of resonance energies.

***PT*-NONINVARIANT CORRELATIONS. INVESTIGATION TECHNIQUES**
Scheme with a circular polarimeter.

This scheme is proposed in [4]. It is based on $(\vec{\sigma}_n[\vec{k}_1 \times \vec{c}_\gamma])$ correlation in (n,γγ)- or similar reactions induced by neutrons. Here $\vec{c}_\gamma$ is circular polarization of second γ-quantum. First transition of the discussed correlation is an object in which ***PT***-noninvariant amplitude is searched for, and the second one is an analyzer. If primary particle is a γ-quantum distribution of the products takes the form:

$$W_{LJF}(\theta_{\gamma_1},\theta_{\gamma_2},\phi_{\gamma_1},\phi_{\gamma_2}) = \sum \rho_j^m(I)\,\varepsilon_{j_{\gamma 1}}^{m_{\gamma 1}} *(L_{\gamma_1} p_{\gamma_1}, L'_{\gamma_1}\, p'_{\gamma_1})$$
$$\varepsilon_{j_{\gamma 2}}^{m_{\gamma 2}} *(L_{\gamma_2} p_{\gamma_2}, L'_{\gamma_2}\, p'_{\gamma_2})\,\varepsilon_{j'}^{m'*}(F)\;\hat{I}^2\hat{J}^2\,(j_{\gamma_1} m_{\gamma_1} j_{\gamma_2} m_{\gamma_2}\,|\,j\,m)$$
$$\begin{Bmatrix} J & L_{\gamma_1} & I \\ J & L'_{\gamma_1} & I \\ j_{\gamma_2} & j_{\gamma_1} & j \end{Bmatrix} \begin{Bmatrix} F & L_{\gamma_2} & J \\ F & L'_{\gamma_2} & J \\ 0 & j_{\gamma_2} & j_{\gamma_2} \end{Bmatrix} \hat{j}_{\gamma_1}\hat{j}_{\gamma_2}^2 \left\langle J \left| L'_{\gamma_1}\, p'_{\gamma_1} \right| I \right\rangle * \left\langle J \left| L_{\gamma_1} p_{\gamma_1} \right| I \right\rangle$$
$$\left\langle F \left| L'_{\gamma_2}\, p'_{\gamma_2} \right| J \right\rangle * \left\langle F \left| L_{\gamma_2} p_{\gamma_2} \right| J \right\rangle. \qquad (3)$$

Here $\hat{b} = \sqrt{2b+1}$; 3×3 table is 9j-syumbol; $\rho_j^m(I)$ is the statistical tensor of a state *I*; $\varepsilon_{j_{ir}}^{m_{ir}}(lp, l'p')$ – efficiency tensor of a detector of irradiated particle; *I* denotes initial compound nucleus state, *J* – intermediate one, and *F* is a final state; $L_{\gamma_i} p_{\gamma_i}, L'_{\gamma_i}\, p'_{\gamma_i}$ – multipolarities of the transitions; $\langle I'|lp|\,I\rangle$ – amplitude of a transition. The sum is over all indexes contained in (3) besides *I, J, F*. The residual nucleus is not registered therefore its efficiency tensor $\varepsilon_{j'}^{m'}(F)$ should be written as:

$$\varepsilon_{j'}^{m'}(F) = \hat{F}\,\delta_{j'0}\,\delta_{m'0}. \qquad (4)$$

If s-resonance absorption is dominating, statistical tensor (rank *j* = 1) produced by the polarized neutron beam takes the form:

$$\rho_{j=1}^0(I) = (1/\sqrt{32\pi})\;\hat{j}\hat{I}_0\;p_z \begin{Bmatrix} I & s & I_0 \\ I & s & I_0 \\ 0 & j & j \end{Bmatrix} \left\langle I \left| j \right| I_0 \right\rangle \left\langle I \left| j \right| I_0 \right\rangle^*. \qquad (5)$$

Here ***s*** = 1/2 is the neutron spin, p_z – the degree of neutron polarization.

The form of the efficiency tensor of a detector of **γ**-radiation insensitive to linear polarization is the following:

$$\varepsilon_{j_\gamma}^{m_\gamma}(lp, l'p') = (1/16\pi)(-1)^{l'-1}\hat{l}\hat{l}'(l1l'-1\,|\,j_\gamma 0)\,[S(0)+S(3))+(-1)^f(S(0)-S(3))]$$
$$(\sqrt{4\pi}/\hat{j}_\gamma)\,Y^*_{j_\gamma m_\gamma}(\theta\varphi), \qquad (6)$$

where $f = (p - p')/2 - j_\gamma$; θ and φ are the angles describing rotation from detector coordinate system to laboratory one; *S(r)* is a Stokes parameter of the detector: *S(*0) is determined by total (including both geometric and physical characteristics) efficiency of registration of unpolarized γ-radiation, and *S(*3) – by total efficiency of detection of its circular polarization including, in addition to the characteristics similar to that of *S(*0), polarization resolution capability.

The angular-dependent part of the expression (3) combined with the formula (5) can be written as:

$$S(3)\sum_{m=-1,1}(1m1-m|10)(\sqrt{4\pi}/\hat{1})Y_1^m(\vec{c}_{\gamma_2})(\sqrt{4\pi}/\hat{1})Y_1^{-m}(\vec{k}_{\gamma_1})=$$

$$(1/\sqrt{2})S(3)\sin(\theta_{\gamma_2})\sin(\theta_{\gamma_1})\sin(\phi_{\gamma_1}-\phi_{\gamma_2}), \qquad (7)$$

thus for the maximum efficiency of the setup directions of the detector axes are bound to be orthogonal to the direction of neutron polarization and to each other as it is demonstrated by fig. 3.

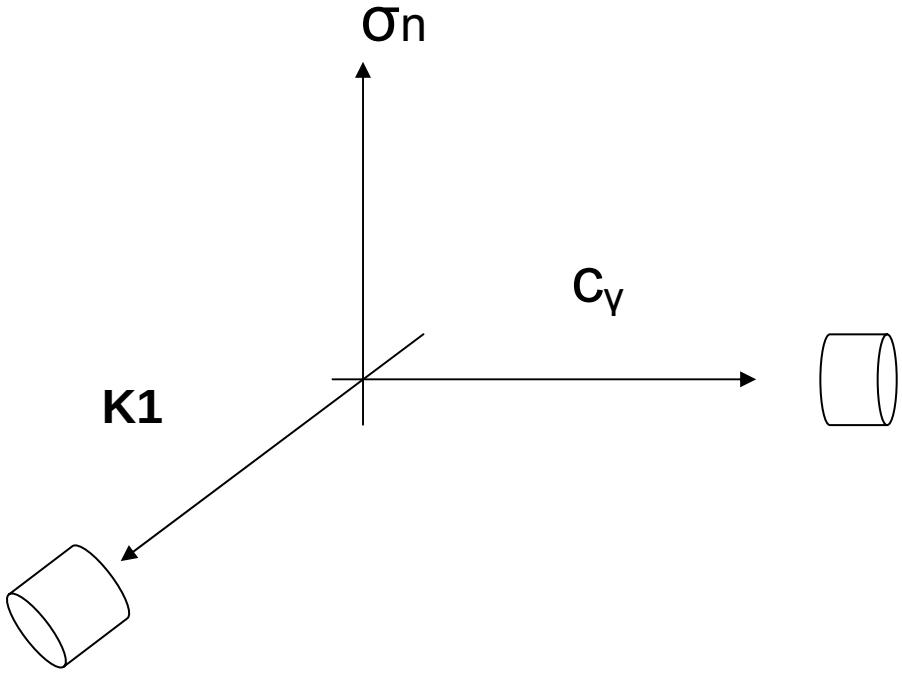

Figure 3. Optimal geometry of the scheme with a circular polarimeter.

The effect is proportional to the difference between the counting rate of coincidences for positive and negative value p_z. In fact to get rid of systematic inaccuracy of measurement scheme one needs in two detector of the first γ-quantum + two detector of the second γ-quantum setup. High-precision goniometry is necessary anyway.

Scheme with a linear polarimeter.

This scheme is proposed in [5] and realized first time in the mentioned above ref. [3]. It is based on the linear polarimetry of radiation of a sample. This approach exploits the correlation $(\vec{k}_\gamma[\vec{\varepsilon}\times\vec{J}])(\vec{J}\vec{\varepsilon})$ where ε – linear polarization of the γ-quantum, J – orientation vector of a source. Square dependence of the correlation on the vector J demonstrates, obviously, that aligned sample is necessary. Cryogenic methods may be used to

create it. Such a sample can also be obtained in capture process of an incident projectile with nonzero angular momentum. The alignment may be visualized by registration of a direction of a particle $\vec{k}_1$, preceding γ-quantum in a cascade. A subsequent particle can also be used for the same purpose. In these three cases the correlation takes the form: $(\vec{k}_\gamma[\vec{\varepsilon}\times\vec{k}_1])(\vec{k}_1\vec{\varepsilon})$, where $\vec{k}_1$ s a direction of a projectile, or a preceding, or a subsequent particle. Naturally measurement of coincidences in the mentioned cascade is necessary.

Formalism of these correlations involves the expression:

$$W_{LF}(\theta_\gamma,\phi_\gamma,\psi_\gamma)=\sum \rho^0_{j_\gamma}(I)\,\varepsilon^{m=0}_{j_\gamma}(L_\gamma p_\gamma, L'_\gamma\, p'_\gamma)\,\varepsilon^{m'*}_{j'}(F)\,\hat{j}_\gamma\,\hat{I}^2 \begin{Bmatrix} F & L_\gamma & I \\ F & L'_\gamma & I \\ 0 & j_\gamma & j_\gamma \end{Bmatrix} \langle F\,|\,L'_\gamma\, p'_\gamma\,|\,I\rangle^*\langle F\,|\,L_\gamma p_\gamma\,|\,I\rangle, \tag{8}$$

which is related to the transition in which PT-noninvariant amplitude is searched for The rank of the statistical tensor j_γ = 2 determines the alignment in this formula.

After a capture of unpolarized particle with the spin *s*=1/2 by a target the tensor takes the following form and satisfies the following conditions:

$$\rho^0_k(I) = (1/4\pi)\sum_{ll'j}(-1)^{l'}\hat{l}\hat{l}'\hat{I}_0\hat{s}^{-1}\hat{k}^3\hat{I}^2\hat{j}\hat{j}'(l0l'0\,|\,k0)\begin{Bmatrix} I & j & I_0 \\ I & j' & I_0 \\ k & k & 0 \end{Bmatrix} \begin{Bmatrix} l & s & j \\ l' & s & j' \\ k & 0 & k \end{Bmatrix}\langle I_0\,|\,j'\,|\,I\rangle^*\langle I_0\,|\,j\,|\,I\rangle;\ k{=}2;\ \mathrm{I}{\geq}1;\ j{=}j'{=}3/2;\ l,l'{>}0 \tag{9}$$

Efficiency tensor of the detector insensitive to the circular polarization can be expressed through the angles between the direction of the alignment of the sample and the direction of the emitted γ quantum θ and φ in the following form:

$$\varepsilon^{m=0}_{j_\gamma}(lp,l'p')=(1/16\pi)ll'\{2(-1)^{l'-1}\,(l1l'-1\,|\,j_\gamma 0)S(0)\,P_{j_\gamma}(\cos\theta)\,+$$

$$p'\sqrt{\frac{(j_\gamma-2)!}{(j_\gamma+2)!}}\,(l1l'1\,|\,j_\gamma 2)\,P^{(2)}_{j_\gamma}(\cos\theta)\,[S(1)(1+(-1)^f)-iS(2)(1-(1)^f)] \tag{10}$$

where $P_{j_\gamma}(\cos\theta)$ is Legendre polynomial, $P^{(2)}_{j_\gamma}(\cos\theta)$ – a joint Legendre polynomial of the second order. Obviously there is no dependence on φ due to the rotational invariance of the set up about the direction of the orientation vector. The Stokes parameters of the linear polarimeter may be expressed as: $S(1)=A\cos 2\psi$, $S(2)=A\sin 2\psi$, where ψ determines the plate of the linear polarization in a certain coordinate system. It is the $\sin 2\psi$-dependent term that is produced by PT-noninvariant amplitudes. Thus the existence of these amplitudes

result in rotation of linear polarization plate with respect to the direction of the alignment: W(ψ)~cos2($\psi-\delta_\psi$). Other terms of (10): scalar one ($j_\gamma = 0$), ψ -independent, and $\cos 2\psi$ -dependent are sources of a strong background in the search for this term. The experimental setup based on Compton linear polarimeter is schematically illustrated by fig. 4. Four-detector scheme is necessary to get rid of systematic inaccuracy of measurement setup.

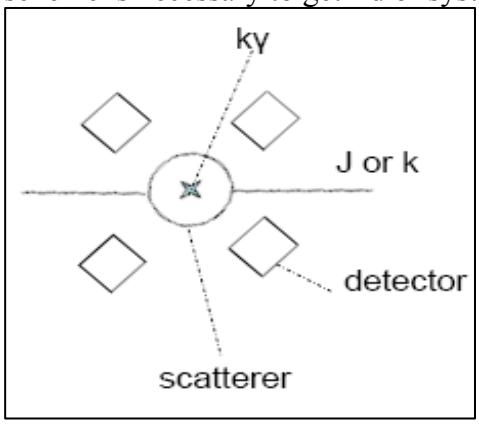

Figure 4. Optimal geometry of the scheme with a linear polarimeter.

The optimal conditions for search for this correlation are obviously the following: the axis of the polarimeter is bound to be orthogonal to the direction of the alignment, four detectors are bound to be located at the directions determined by the azimuthal angles: $\psi = \pm\pi/4$, $\psi = \pm 3\pi/4$ as it is shown in fig. 4. Polar angles are determined by Compton scattering cross section maximum. High-precision goniometry of the setup is necessary again.

Coincidence scheme as a polarimeter

This scheme was realized in [2]. In contrast to the just discussed one, coincidences of γ-quanta of the cascade produced by the aligned source are used as an analyzer of linear polarization. Thus the following correlations fall into this pattern: $(\vec{k}_{\gamma_1} \cdot [\vec{J} \times \vec{k}_{\gamma_2}])(\vec{k}_{\gamma_2} \cdot \vec{J})$; $(\vec{k}_{\gamma_1} \cdot [\vec{k}_1 \times \vec{k}_{\gamma_2}])(\vec{k}_{\gamma_2} \cdot \vec{k}_1)$. One of two γ-transitions of the discussed cascade (it is denoted γ_1 in the notations of the correlations being the first or the second in the cascade) is an object in which PT-noninvariant amplitude is searched for, and the other one plays a role of an analyzer. The expression of the correlation is the same as in the scheme with the circular polarimeter:

$$W_{LJF}(\theta_{\gamma_1},\theta_{\gamma_2},\phi_{\gamma_1},\phi_{\gamma_2}) = \sum \rho_j^0(I)\, \varepsilon_{j_{\gamma_1}}^{m_{\gamma_1}*}(L_{\gamma_1} p_{\gamma_1}, L'_{\gamma_1}\, p'_{\gamma_1})$$
$$\varepsilon_{j_{\gamma_2}}^{m_{\gamma 2}*}(L_{\gamma_2} p_{\gamma_2}, L'_{\gamma_2}\, p'_{\gamma_2})\, \varepsilon_{j'}^{m'*}(F)\ \hat{I}^2 \hat{J}^2\, (j_{\gamma_1} m_{\gamma_1} j_{\gamma_2} m_{\gamma_2} | j\, 0)$$
$$\begin{Bmatrix} J & L_{\gamma_1} & I \\ J & L'_{\gamma_1} & I \\ j_{\gamma_2} & j_{\gamma_1} & j \end{Bmatrix} \begin{Bmatrix} F & L_{\gamma_2} & J \\ F & L'_{\gamma_2} & J \\ 0 & j_{\gamma_2} & j_{\gamma_2} \end{Bmatrix} \hat{j}_{\gamma_1} \hat{j}_{\gamma_2}^2 \langle J | L'_{\gamma_1}\, p'_{\gamma_1} | I \rangle^* \langle J | L_{\gamma_1} p_{\gamma_1} | I \rangle$$
$$\langle F | L'_{\gamma_2}\, p'_{\gamma_2} | J \rangle^* \langle F | L_{\gamma_2} p_{\gamma_2} | J \rangle, \qquad (11)$$

however the discussed correlations are characterized by other tensor properties: $j_{\gamma_1}=1; j_{\gamma_2}=2; j=2$. Statistical tensor has the form (9) here. Efficiency tensor of the detectors insensitive to the linear and/or the circular polarization which are required in the discussed scheme can be expressed as:

$$\varepsilon_{j_\gamma}^{m=0}(lp,l'p')=(1/16\pi)ll'\{2(-1)^{l'-1}(l1l'-1|j_\gamma 0)S(0)P_{j_\gamma}(\cos\theta). \quad (12)$$

The optimal location of the detectors is similar to the one used in the scheme with linear polarimeter (fig. 4) if the scatterer is replaced by the detector of γ_1 in it and axises of the detectors are directed not to the scatterer but to the sample .

Methods of preparation of oriented samples

Method of preparation of polarized sample by use of polarized neutron beam is effective and useful. It is appropriate for s-wave neutron reactions. Direction of the polarization is simply reversed.

The alignment may be obtained by action of a strong magnetic field on the target sample mounted in deep cryogenic conditions. The orientation vector of a source *J* is directed parallel or antiparallel to the direction of the magnetic field. Alternative way to obtain the alignment is the registration, besides the studied γ-quantum, a preceding or a subsequent particle of a cascade, or it may appear as a consequence of the capture of an incident projectile with nonzero angular momentum (p-neutron for example). S-neutrons are invalid to prepare aligned sample.

FEATURES OF NEAR-P-RESONANCE NEUTRON EXPERIMENTS

Search for P-violation

As it was pointed out above the basic condition to obtain a low upper limit of a PT-noninvariant effect is a manifestation of a sufficiently strong P-violation effect in the chosen example. Elastic neutron scattering at p-resonance energy produces great P-odd correlations. It displays longitudinal analyzing power ($10^{-2.5} \div 10^{-1}$) in neutron transmission and total cross section experiments. Unfortunately realization of the idea to use the elastic neutron scattering from polarized La target for search for PT-noninvariant effect (La experiment) met great obstacles due to the simulation effect originated by the final state interaction.

What about (n,γ)-reactions it is known that for certain samples these reactions induced by thermal neutrons result in values of circular polarization of γ-radiation P_γ and asymmetry of γ-radiation of a polarized sample A_γ which are not small ($10^{-3.5} \div 10^{-2.5}$) but essentially lower in comparison with just discussed. What is E-dependence of the effects?

To estimate P-violation effects in near-resonance (n,γ)-processes we use the formula directly derived from expression presented in [6] if one ***s***-wave and one ***p***-wave resonances are taken into account:

$$P_\gamma(A_\gamma)=2\frac{F_{\{s\}}^{pv}\sqrt{\Gamma_p^\gamma/\Gamma_s^\gamma}(E-E_p)+F_{\{p\}}^{pv}(\Gamma_p^n/\Gamma_s^n)(\sqrt{\Gamma_p^\gamma/\Gamma_s^\gamma})(E-E_s)}{(E-E_p)^2+\Gamma_p^2/4+[(E-E_s)^2+\Gamma_s^2/4](\Gamma_p^n/\Gamma_s^n)(\Gamma_p^\gamma/\Gamma_s^\gamma)}\times \quad (13)$$

$$<J_c(p)|V_{pv}|J_c(s)>;$$

where $|J_c>$ is a wave function of a compound state, J_c – the spin of the respective compound-resonance, V_{pv} – the potential of parity violation, Γ^n, Γ^γ, and Γ with the indicated resonance indexes denote neutron, gamma, and total resonance widths respectively, spin factors $F_{\{s\}}^{pv}, F_{\{p\}}^{pv}$ denote elements of Racah algebra peculiar for investigated P-odd

correlations. Here we omit the factor, which take into account the contribution of $p_{3/2}$ channel for brevity. Gamma-transition to a certain level of residual nucleus is meant in the formula.

Let us consider a near-p-resonance energy point *E* ($E - E_p >> E - E_s$). Presence of an extremely small factor $(\Gamma_p^n / \Gamma_s^n)$ contained in the second summand of the numerator allows one to neglect this summand. So do the summand $\Gamma_s^2 / 4$ in the denominator. After that the location of the maximum of the curve of E-dependence of the effect E_m is easily found:

$$E_m - E_p = \sqrt{\Gamma_p^2 / 4 + (E_m - E_s)^2 (\Gamma_p^n / \Gamma_s^n)(\Gamma_p^\gamma / \Gamma_s^\gamma)}, \tag{14}$$

and its value can be expressed as:

$$P_\gamma^m (A_\gamma^m) = \frac{F_{\{s\}}^{pv} < J_c(p) | V_{pv} | J_c(s) > \sqrt{\Gamma_p^\gamma / \Gamma_s^\gamma}}{\sqrt{\Gamma_p^2 / 4 + (E_m - E_s)^2 (\Gamma_p^n / \Gamma_s^n)(\Gamma_p^\gamma / \Gamma_s^\gamma)}}. \tag{15}$$

Phenomenology of rather heavy (A>90) nuclei demonstrates that ordinary the width of p-resonance $\Gamma_p < 2(E_p - E_s)\sqrt{(\Gamma_p^n / \Gamma_s^n)}$ although it may be of the same order of magnitude. Therefore it is useful to present the formula (15) as:

$$P_\gamma^m (A_\gamma^m) = B \frac{F_{\{s\}}^{pv} < J_c(p) | V_{pv} | J_c(s) >}{E_m - E_s} \sqrt{(\Gamma_s^n / \Gamma_p^n)}, \tag{16}$$

for ***γ***-transitions fulfilling the condition $\sqrt{\Gamma_p^\gamma / \Gamma_s^\gamma} \geq 1$ the multiplier *B* has the form and the value:

$$B = \frac{(E_m - E_s)\sqrt{(\Gamma_p^n / \Gamma_s^n)(\Gamma_p^\gamma / \Gamma_s^\gamma)}}{\sqrt{\Gamma_p^2 / 4 + (E_m - E_s)^2 (\Gamma_p^n / \Gamma_s^n)(\Gamma_p^\gamma / \Gamma_s^\gamma)}} \approx 1 \tag{17}$$

In the same energy region the expression of longitudinal analyzing power of the elastic scattering has the form:

$$A_n = \frac{-2F_{\{n\}}^{pv} < J_c(p) | V_{pv} | J_c(s) > \sqrt{\Gamma_p^n / \Gamma_s^n}[E - E_p + (E - E_s)(\Gamma_p / \Gamma_s)]}{(E - E_p)^2 + \Gamma_p^2 / 4 + [(E - E_s)^2 + \Gamma_s^2 / 4](\Gamma_p^n / \Gamma_s^n)(\Gamma_p / \Gamma_s)}. \tag{18}$$

In the resonance point, by neglecting the same summands as in (13), the following formula for the maximal value of longitudinal analyzing power may be obtained:

$$A_n^m = -2B' \frac{F_{\{n\}}^{pv} < J_c(p) | V_{pv} | J_c(s) >}{E_p - E_s} \sqrt{\Gamma_s^n / \Gamma_p^n}, \tag{19}$$

where the multiplier *B'* differs from *B* by the replacements: $\Gamma_p^\gamma \to \Gamma_p, \Gamma_s^\gamma \to \Gamma_s$. Ordinary it is also close to unity.

So with no regard for the small difference of the values $E_p - E_s$ and $E_m - E_s$ a simple relation may be obtained:

$$P_\gamma^m(A_\gamma^m) = -\frac{B}{2B'}(F_{\{s\}}^{pv} / F_{\{n\}}^{pv}) A_n^m . \qquad (20)$$

The values of the spin factors $F_{\{s\}}^{pv}, F_{\{n\}}^{pv}$ depend on the type of correlation, multipolarity of the γ-transitions, and the spin of a target nucleus, however in most cases they lie in the range $10^{-1} \div 10^{0}$. Thus it may be concluded that maximal values of P-odd observables of (n,γ)-reactions are roughly the same as the resonance neutron scattering ones. As it is seen from (14) location of a maximum depends on the choice of γ-line. Anyway expression (20) pointes very useful way to estimate the discussed P-odd observables and demonstrates promising prospect of search for P-odd effects of very high values in (n,γ)-reactions. In addition the expression (20) provides a very convenient way to estimate them using, for example, the data from the review [7] or other data concerning P-odd neutron scattering.

Presented estimates may be confirmed and extended on the base of experimental data obtained in the measurements of the values P_γ and A_γ which use thermal neutron beam [8-10]. Using exp. (16) with the replacement $E_m - E_s \to E_p - E_s$ and the exp. (13) in which the second and third summands of the denominator are neglected one may write:

$$P_\gamma^m(A_\gamma^m) = \frac{(E_{th} - E_p)}{2(E_p - E_s)\sqrt{(\Gamma_p^n / \Gamma_s^n)(\Gamma_p^\gamma / \Gamma_s^\gamma)}} P_\gamma^{th}(A_\gamma^{th}), \qquad (21)$$

E_{th} is the thermal neutron energy here. Basing on the data presented in [8 – 10] and the exp. (21) it may be concluded that typical values near-p-resonance P-odd effects is in the neighborhood of $1 \cdot 10^{-2}$.

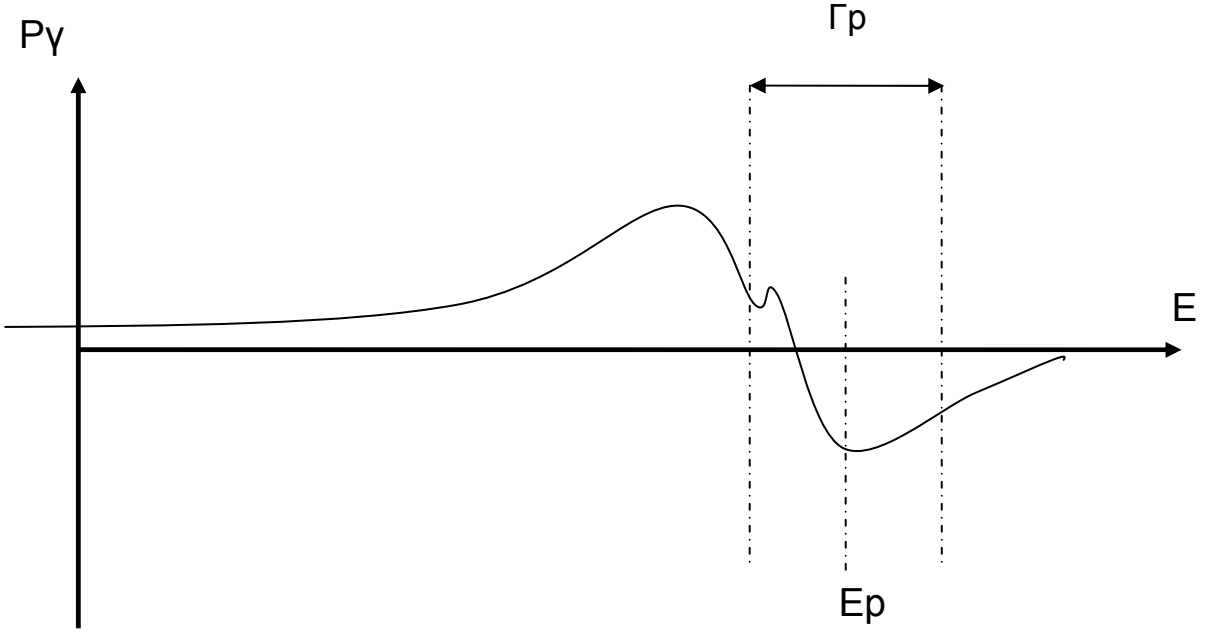

*Figure 5. Energy dependence of **P**-odd effect.*

A behavior of P-odd effects peculiar for (n,γ)-reactions is schematically presented in the fig. 5. Small peak is the manifestation of p-wave term appearing due to the second summand of the numerator of (13). Time of flight method is convenient to measure presented curve as a whole. All energy bins and all promising γ-lines may be analyzed simultaneously.

PT-nonconservation in near-*p*-resonance energy regions

Great values of P-odd observables typical for the discussed processes in near-p-resonance regions give grounds to expect that the same sample turn out to be promising in the study of PT-nonconservation in the (n,γ)-reactions. Simple rearrangement of the formalism presented in [6] result in the following expression of a PT-nonconserving effect:

$$a_{pt} = \frac{< J_c(p) \mid V_{ptnc} \mid J_c(s) > \sqrt{\Gamma_p^\gamma / \Gamma_s^\gamma}\,[F_{\{s\}}^{ptnc}\Gamma_p + F_{\{p\}}^{ptnc}\Gamma_s(\Gamma_p^n / \Gamma_s^n)]}{(E-E_p)^2 + \Gamma_p^2/4 + [(E-E_s)^2 + \Gamma_s^2/4](\Gamma_p^n/\Gamma_s^n)(\Gamma_p^\gamma/\Gamma_s^\gamma)}. \qquad (22)$$

Introducing the approximations discussed above one may rewrite the exp. (22) at the resonance point in the form:

$$a_{pt}^m = B^2 \frac{< J_c(p) \mid V_{ptnc} \mid J_c(s) > F_{\{s\}}^{ptnc}\Gamma_p}{(E-E_s)^2(\Gamma_p^n/\Gamma_s^n)\sqrt{\Gamma_p^\gamma/\Gamma_s^\gamma}}. \qquad (23)$$

Because of the great body of available data concerning P-odd effect in neutron elastic scattering to estimate capabilities of various examples of ***p***-resonances in search for PT-noconservation it is convenient to compare (23) and (19). This procedure results in the formula:

$$a_{pt}^m = \frac{B^2 < J_c(p) \mid V_{ptnc} \mid J_c(s) > F_{\{s\}}^{ptnc}\Gamma_p \sqrt{(\Gamma_s^n/\Gamma_p^n)}}{2B' < J_c(p) \mid V_{pv} \mid J_c(s) > F_{\{n\}}^{pv}(E_p - E_s)\sqrt{\Gamma_p^\gamma/\Gamma_s^\gamma}} A_n^m. \qquad (24)$$

If, fortunately, appropriate γ-line with the widths satisfying the condition:

$$\sqrt{\frac{\Gamma_p^\gamma}{\Gamma_s^\gamma}} \approx \frac{\Gamma_p \sqrt{\Gamma_s^n / \Gamma_p^n}}{(E_p - E_s)} \qquad (25)$$

would be found then the formula (24) takes the form:

$$\alpha_{PT}^m \approx \frac{\left\langle J_c(p) \middle| V_{PTNc} \middle| J_C(s) \right\rangle F_{\{S\}}^{PTNC}}{2B' \left\langle J_c(p) \middle| V_{PV} \middle| J_c(s) \right\rangle F_{\{n\}}^{PV}} A_n^m \qquad (26)$$

For γ-lines with the widths ratio different from (25) the ratio a_{pt}^m / A_n^m is slightly smaller.

Energy dependence of a PT-nonconservation effect (22) is schematically shown in the fig. 6. (thick dashed line) together with the curve of the P-odd effect (scales are chosen arbitrary). The latter one is presented for discussion of a false effect of initial state interaction (ISI) simulating the PT-noninvariant effect. The matter is that not only final state interaction but also ISI results in phase shift which simulates P-even T-noninvariant effect. Therefore this false effect, together with the actual P-violation one, result in simulation of a PT-

nonconservation correlation related to one of the presented above types. Energy dependence of this false effect in the resonance region is similar to the dependence of ***P***-odd effect. Fortunately phase shifts of p- and s-waves are small at low neutron energy. For ***s***-wave for example:

$$\delta_S = kR_{nucleus} \approx 2 \cdot 10^{-3} \tag{27}$$

for E =1 eV. In addition the shape of the false effect curve is differs strongly from the curve of actual ***PT***-nonconserving one maximum of which is placed in the resonance point where false effect is small. Due to that the problem of the background seems to be not drastic. Moreover a measurement of the false effect may be a very good test of experimental setup.

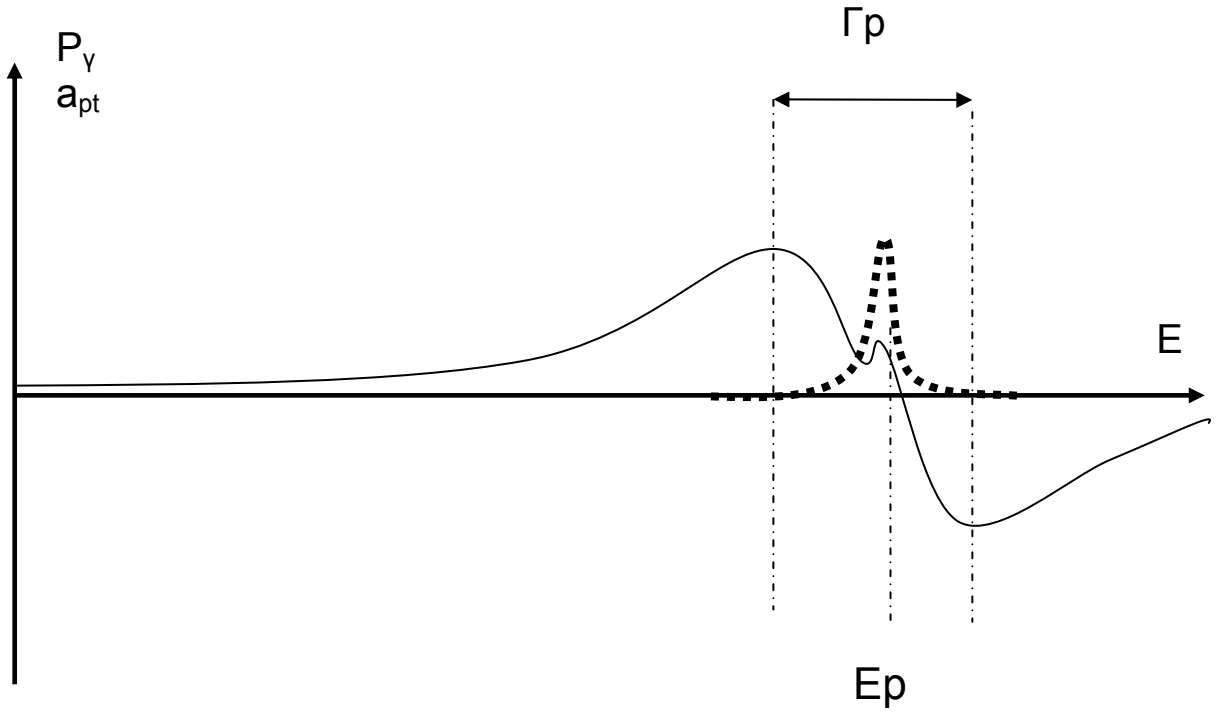

*Figure 6. Energy dependence of **PT**-nonconservation effect.*

Coming back to the choice of optimal experimental approach let us discuss peculiarities of the measuring schemes.

Advantage of the scheme based on the circular polarimeter is relatively easy method of orientation of the sample using polarized neutron beam. The sign of polarization of the sample is changed by a flipper. Disadvantages of the scheme are the necessity in use of coincidence scheme which strongly limit the counting rate and very low (few per cent) polarization resolution capability of the circular polarimeter loosely dependent on γ-quantum energy.

The second scheme basing on the linear polarimeter is the sole one in which one can get rid of a coincidence scheme. It may be done at p-resonance energy. The rotation of linear polarization plate with respect to the direction of the alignment may be detected using two scatterers of the type presented in fig. (4) placed specularly. Even more reliable approach is to measure γ-radiation of two p-resonances close in energy scale one of which demonstrates a strong P-odd correlation and another one does not. Disadvantage of this variant is that as it was shown above PT-nonconserving effect is relatively weak in p-wave amplitude and s-wave amplitude does not produce the alignment.

The alignment of the sample populated by s-wave in which the maximal effects are expected may be obtained by use of a coincidence scheme of orientation. This method, as it was mentioned above, puts a serious limitation on the counting rate. An alternative way is to use a refrigerator. However it is possible to achieve high degree of alignment by cryogenic means for the limited list of targets.

Another disadvantage of the discussed scheme is low polarization resolution capability of the linear polarimeter at high (several MeV) energy γ-quantum region which is approximately of the same order of magnitude as circular polarization one. And it is this region typical for energies of primary γ-transitions in which one can expect strong effects under discussion in (n,γ)-reactions.

The third measuring method is free of the last disadvantage but one must use some coincidence scheme (in one of the presented above versions – triple) again. At the same time it is the sole scheme in which polarimetry is not required.

For all presented correlations the interference between γ-transition amplitudes which differ in phase by the value $\pi/2$ is necessary. In the (n,γ)-reactions primary E1- or M1-transitions are dominating almost without exception. Therefore in the most cases only these amplitudes provide a chance to search for the discussed correlations. However the values of correlation coefficients expressed by the formulas (3) and (11) turn out to be zero for E1+M1 interference terms due to the properties of first 9j-symbols contained in the expressions. So the only untypical E1+E2 interference terms are contributable in the correlations. The sole exception is the second scheme. That is why it is reasonable to consider the scheme with a linear polarimeter as the basic. Naturally the choice of optimal experimental approach depends on a particular example and exclusions in which one of two other schemes is preferable may be found.

SUMMARY AND CONCLUSIONS

Summing up presented above discussion it is important to stress the following essential points:

1. Study of (n,γ)-reactions in near-p-resonance energy regions looks a promising line in search for great P-violation effects and low upper limits of PT-nonconservation effects in nuclei.

2. In fact s-wave amplitude in the entrance channel makes a dominating contribution to both effects without exceptions.

3. Investigations of P-violation effects using such an approach are of interest due to their great values.

4. The experimental scheme based on a cryogenic method of orientation of a target and the measurement of linear polarization of emitted γ-quanta offer obvious advantages over other ones and it is reasonable to consider it as a basic.

5. The choice of optimal target for the study of PT-nonconservation effect significantly depends on: the value of the P-violation effect, existence of appropriate γ-line(-s), possibility to prepare the aligned target by cryogenic means.

6. Some versions of the approach aimed to search for PT-invariance break up are capable to reduce upper limit of the effect achieved recently in nuclear experiments by several orders of magnitude.

ACKNOWLEGEMENTS

Authors express their gratitude to a wide group of participants of LNF seminar and personally to L.B. Pikel'ner, E.I. Sharapov, V.I. Furman, Yu.N. Kopach, L.V. Mitsyna, S.S. Parzicki, P.V. Sedyshev for fruitful discussions and recommendations.

REFERENCES

1. V.G. Nikolenko et al. In: Proceedings of ISINN - 15, Dubna, JINR, 2008. P. 304.
2. T. Murdoch et al. Phys. Lett. 1974. V. B 52. P. 325.
3. V.G. Tsinoev et al. Phys. At. Nucl. 1998. V. 61. P. 1357.
4. I.S. Okunev, Yu. M. Tchuvil'sky. In: Proceedings of ISINN - 10, Dubna, JINR, 2003, P. 44.
5. Z. Szymanski. Nucl. Phys. 1968. V. A113. P. 385.
6. O.P. Sushkov, V.V. Flambaum. Preprint of INP Siberian division of AS 83-97, Novosibirsk, 1983.
7. G.E. Mitchell, J.D. Bowman, S.I. Penttila, E.I. Sharapov. Phys. Rep. 2001. V. 354. P. 157.
8. L.M. Smotritsky, V.N. Dobrynin. Preprint PNPI-2041, Gatchina, 1995.
9. V.A. Vesna et al. JETP Lett. 1982. V. 36. P. 169.
10. A.I. Egorov et al. Preprint LNPI-1067, Leningrad, 1985.